Picosecond burst pulse machining with temporal energy modulation [Invited]

Akinao Nakamura[1], Tomoki Mizuta[1], Yasuhiko Shimotsuma[1,*], Masaaki Sakakura[1], Tomohito Otobe[2], Masahiro Shimizu[1], and Kiyotaka Miura[1]

[1]*Department of Material Chemistry, Graduate School of Engineering, Kyoto University, Kyoto 615-8510, Japan*
[2]*National Institutes for Quantum and Radiological Science and Technology, Kansai Photon Science Institute, Kyoto 619-0215, Japan*
**Corresponding author: yshimo@func.mc.kyoto-u.ac.jp*

Received June 9, 2020; accepted August 11, 2020; posted online September 27, 2020

Suppression of stress and crack generation during picosecond laser processing in transparent brittle materials such as glass was successfully demonstrated by a picosecond laser pulse with temporal energy modulation. The origin of deterioration in processing accuracy could be interpreted in terms of the discontinuous movement of plasma in the vicinity of the focus. To reveal the effectiveness of the temporal energy modulation for smooth machining, such plasma motion was simulated by the finite-difference time-domain method. Furthermore, photoinduced birefringence was observed using a high-speed polarization camera.

Keywords: picosecond laser; energy modulation; burst pulse; material processing; stress distribution.
doi: 10.3788/COL202018.123801.

Over the past few decades, direct laser writing using ultrafast laser pulses has attracted attention in a wide field ranging from photosynthesis, solar power generation, optical storage, to surgery. In particular, laser machining has been an indispensable tool for the industrially relevant applications of smart manufacturing such as mobile electronic devices, displays, and semiconductors. In general, laser machining, which has a high spatial and temporal coherence and high power density, is used for cutting, drilling, welding, and hardening, or photochemical reactions leading to etching and deposition. Therefore, even today, a light source with a high flexibility in beam parameters such as wavelength, power, power density, temporal waveform, and spatial profile is developed. From the viewpoint of the diffraction limit, a deep-UV laser, and from the viewpoint of nonlinear optics, an ultrashort pulse laser have already been put to practical use. More recently, the ultrashort pulsed laser with a high repetition rate has been attracting much interest as a tool for local melting[1–4] and micro-welding of transparent materials such as glass[5–8]. Such local melting is triggered by nonlinear photoexcitation and successive local heat accumulation[9]. For laser welding, local melting is induced at the interface between two substrates. Because the molten region is confined by solid materials, the thermal damage, which often occurs on a free surface of a solid, can be minimized[4]. Therefore, laser welding by an ultrashort pulsed laser has an advantage compared to a universal technology for wafer level packaging using adhesives or glass frits[10]. It is known that the internal modification mechanism changes depending on the pulse width[11]. Such dependence on the pulse width can be interpreted in terms of the photoexcitation and subsequent nonlinear absorption[12]. Nonlinear photoexcitation processes such as multiple-photon excitation are dominant for shorter pulse widths, while absorption by excited electrons increases as the pulse width becomes longer because of a longer interaction time. Recently, Miyamoto *et al.* reported that the nonlinear absorption process by the thermally excited electrons becomes dominant during local melting induced by longer laser pulses with high repetition rates[13]. The periodic and discontinuous movement of highly absorptive plasma in the laser propagation direction during laser welding, leading to the formation of the discontinuous modified region[14,15], was also observed. Consequently, it could be possibile that such a discontinuous modification is causing the problem of irregular stress distribution. Although a picosecond laser pulse system is more attractive for industrial applications due to its compactness and low cost compared to a femtosecond laser system, it should overcome such disadvantages to form homogeneous modification.

Previously, we have reported that the smoothness of the modified region in alkali silicate glass is completely different depending on the pulse width. While the modification induced by 100 fs laser pulses was smooth, the irregular structures and the randomly curved boundaries were formed by 10 ps laser pulses. We have also proposed a method to suppress the stress distribution during laser writing in glass by temporally modulating the pulse energy of picosecond laser pulses[16]. We found that the irregular stress concentration can be suppressed, leading to an enhanced energy threshold for crack generation in glass. In this paper, we observed the difference in the plasma movement during picosecond laser writing with and without the temporal modulation of pulse energy using a high-speed camera. Assuming the generated plasma acts as a complete conductor, we also simulated the plasma motion based on the calculated electric field component. Furthermore, by using a high-speed camera equipped with a pixelated polarizer array made from a

photonic crystal bonded directly to the CMOS sensor, we also performed the time-resolved observation of the stress distribution caused by the plasma movement. Based on the observed phenomena, we discussed the mechanism of the suppression of the stress distribution by the temporal energy modulation of picosecond laser pulses.

In the experiments, we used a picosecond pulsed laser system of a diode-pumped $Nd:YVO_4$ laser (Atlantic; EKSPLA) as a laser source. The wavelength and pulse width were 1064 nm and 10 ps, respectively. The laser pulses were focused inside an alkali silicate glass plate placed on an *XYZ* translation stage (ALIO Industries) with a 20× objective (NA 0.45, CFI LU Plan EPI; Nikon). During laser irradiation, the glass plate was translated perpendicularly to the laser focusing axis to form a modified region. The typical pulse repetition rate and writing speed were set to be 500 kHz and 10 mm/s, respectively. The basic properties of the alkali silicate glass sample are similar to those of soda lime glass. The thickness of the glass sample was 400 μm, and the focus of the laser pulses was about 375 μm below the top surface. The pulse energy was modulated by the external control of the acousto-optic modulator in the picosecond laser system by inputting a voltage waveform (RF signal) from an arbitrary waveform generator (SDG5082; SIGLENT) through an SMA cable. Since the modulation function was set to be typically sinusoidal with a frequency of 1 kHz, the one sinusoidal peak was composed of the energy-modulated 500 pulses [Figs. 1(a) and 1(b)].

In the experiments of the temporal energy modulation, the time-averaged pulse energy was typically set to be 5 μJ. For comparison, the conventional laser experiments (pulse energy: 5 μJ) without energy modulation were also performed. The detailed experimental setup is given

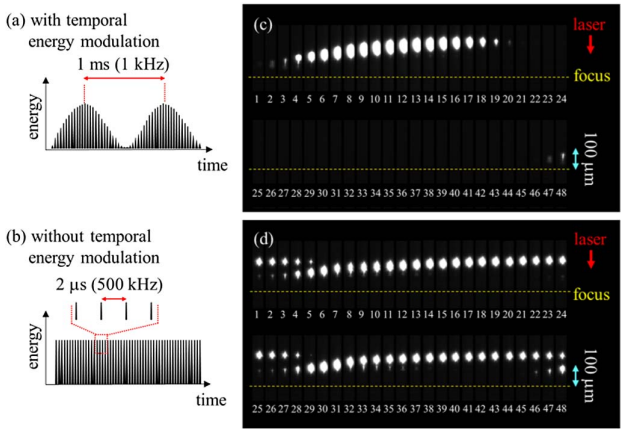

Fig. 1. Schematics of pulse trains (a) with and (b) without temporal pulse energy modulation. Sequential snapshots of plasma in alkali silicate glass induced by picosecond laser irradiation (c) with and (d) without temporal pulse energy modulation. The 48 snapshots with a frame rate of 45,000 fps were taken from the direction perpendicular to the laser propagation. The time-averaged pulse energy was set to be 5 μJ. Yellow dotted lines represent the geometrical focus.

elsewhere[16]. The plasma at the vicinity of the focus during laser writing was observed from the direction perpendicular to the laser focusing axis through a 20× objective (NA 0.40, CFI LU Plan EPI ELWD; Nikon) by using a high-speed camera with a frame rate of 45,000 fps (frames per second) (Fastcam; Photron). Furthermore, by using a high-speed camera (10,000 fps, Crysta; Photron) equipped with a pixelated polarizer array that is made from a photonic crystal bonded directly to the CMOS sensor, we also performed the time-resolved observation of the stress distribution. The wavelength of the illumination light source was 530 nm and was converted to circular polarization by passing through a quarter waveplate. The time-resolved birefringence distribution was observed from the direction parallel to the laser focusing axis through the dichroic filter (DIF-50S-GRE; Sigma-koki).

Figures 1(c) and 1(d) show the sequential snapshots of plasma in a glass sample induced by picosecond laser irradiation with and without pulse energy modulation. The 48 snapshots with a frame rate of 45,000 fps were taken from the direction perpendicular to the laser focusing axis. The time-averaged pulse energy was set to be 5 μJ. Yellow dotted lines represent the geometrical focus. These results clearly indicated that the plasma emission was initially observed slightly above the geometrical focus of picosecond laser pulses, and then gradually moved upward in the laser propagation direction. Such plasma movement during laser irradiation was periodically repeated in both experiments with or without temporal energy modulation. This periodic plasma movement along the laser propagation direction is considered to be due to the thermal lens effect[17–19]. However, there were two distinct differences. One is continuity of plasma generation. In the case without energy modulation, the plasma emission was continuously observed in all the frames [Fig. 1(d)]; on the other hand, the plasma was intermittently generated during laser focusing with energy modulation [Fig. 1(c)]. In the case with energy modulation, the plasma appeared during 20 frames corresponding to about 0.4 ms, and then was not observed between 28 frames (~0.6 ms). It should be noted that in the experiments, 45 frames were recorded during the one sinusoidal peak. Namely, the integrated image of the plasma induced by 11 shots was obtained for each frame, since the shutter speed was set to be 22 μs. Assuming the plasma generation can be observed when the plasma density exceeds a threshold during energy modulation, the peak of the pulse envelope is roughly located in the 11th frame. To produce plasma by the laser irradiation, the pulse energy should reach the energy level corresponding to the threshold of the plasma formation during a time shorter than the plasma lifetime[20,21]. It has been reported that the average lifetime of laser-induced plasma in alkali silicate glass was 100 ps when the plasma density is about 10^{20} cm^{-3}[22,23]. Therefore, spatiotemporal plasma evolution and extinguishment can be obtained in this observation[21].

The other is the multiple plasma formation. In the case without energy modulation, one can see the two spots of

plasma formation during a certain 5 frames (~0.1 ms) every 18 frames (~0.4 ms). Figure 2(a) shows plots of the movement cycle of plasma in a glass sample induced by picosecond laser irradiation with and without energy modulation. In the case without energy modulation, no apparent regularity between the laser pulse repetition rate and the plasma movement cycle was observed. The plasma movement cycle did not change in the case with energy modulation of the 1 kHz sinusoidal wave, even if the laser pulse repetition rate was changed. We have also confirmed that the movement cycle of the plasma is equal to the energy modulation frequency of the sinusoidal wave [Fig. 2(b)]. These results clearly indicate that the plasma was formed at the point when the energy exceeded a threshold during the pulse energy modulation. On the other hand, it is assumed that in the case without energy modulation, since the energy constantly exceeds a threshold in this experimental condition, the multiple plasma formation was observed according to the thermal lens effect. Since the laser writing speed and the pulse repetition rate were 10 mm/s and 500 kHz, respectively, the traveling distance of the laser focus between each pulse was estimated to be 20 μm. Therefore, such apparent differences in the plasma formation with or without energy modulation clearly indicated that the multiple spots of plasma are not due to the integrated images during the shutter speed.

The regions where plasma was generated are considered to be strongly stressed, so the continuity of plasma generation in the case without pulse energy modulation causes the stress accumulation around these regions. However, although such continuity of plasma generation can also be observed for femtosecond laser irradiation, it is known that the modified regions by the femtosecond laser pulses generally exhibit smoothness[24]. It is well known that for pulses longer than a few tens of picoseconds, the generally accepted scenario of laser-induced damage involves the heating of conduction band electrons and transfer of the laser energy to the lattice[12,25]. Damage occurs via conventional heat deposition resulting in the melting and boiling of the material. To reveal the difference in the modification induced by the different pulse widths, we also performed laser writing experiments using a femtosecond laser system with a pulse width of 400 fs and a wavelength of 1035 nm (Monaco; Coherent). The pulse repetition rate was set to 500 kHz. To estimate the stress distribution, the laser-modified regions were inspected using an optical microscope and a polarization microscope (LC-Polscope, CRi). The optical micrographs and the profiles of the phase retardation of modified tracks in alkali silicate glass sample written by laser pulses with different pulse widths are shown in Fig. 3. Since the phase retardation of birefringence is proportional to the stress, the distribution of the phase retardation reflects the stress distribution. Despite that the experimental parameters such as the pulse energy, the pulse repetition rate, and the laser focusing condition are the same except for the pulse width, the stress distribution changed depending on the pulse width. In particular, the phase retardation at the center of the modified region for the pulse width of 10 ps [Fig. 3(e)] was steeply increased and approximately 1.6 times larger compared to that for 400 fs [Fig. 3(d)]. Such differences in the stress concentration could be related to the pressure wave generation[26]. On the other hand, although the intermittent modification was formed in the case of 10 ps pulses with energy modulation [Fig. 3(c)] compared to that for 400 fs [Fig. 3(a)], by the pulse energy modulation, a similar stress distribution to 400 fs was obtained even for 10 ps [Fig. 3(d) and 3(f)].

To reveal the relaxation of the stress concentration at the center of the modified region by 10 ps pulses with energy modulation, we directly observed the time-resolved birefringence distribution during picosecond laser irradiation with and without energy modulation using a high-speed camera equipped with a pixelated polarizer array. The frame rate and the shutter speed were set to be 100 μs. Since the laser writing speed was 10 mm/s, the state of the stress accumulation during 50 pulses every frame can be observed. Figure 4 shows a graph of time-resolved phase retardation at the center of the modified region during laser irradiation. The plot of phase

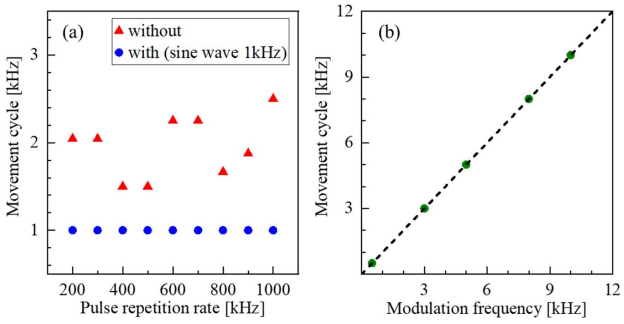

Fig. 2. (a) Plots of the movement cycle of plasma in an alkali silicate glass sample induced by picosecond laser irradiation with and without pulse energy modulation. (b) Plots of the movement cycle of plasma during laser irradiation with pulse energy modulation in a shape of sine wave with various frequencies. The dashed line of $y = x$ is for an eye guide.

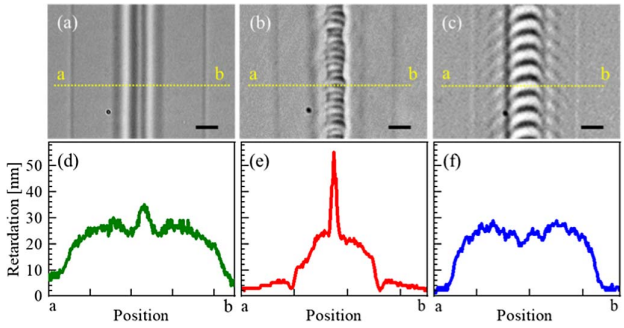

Fig. 3. Optical micrographs of modified tracks in an alkali silicate glass sample written by laser pulses with different pulse widths of (a) 400 fs and (b), (c) 10 ps. The pulse energy modulation was performed for writing the tracks in (c). The profiles of the phase retardation along the dotted yellow lines are also shown in (d)–(f). The scale bar shows 20 μm.

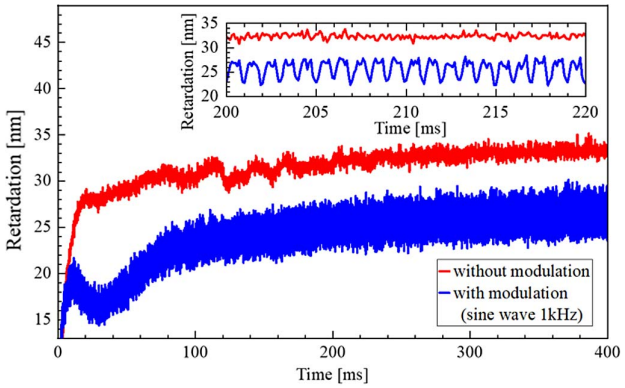

Fig. 4. Time-resolved observation of the phase retardation around the focus of the picosecond laser pulses with and without pulse energy modulation. The inset shows the magnified plots ranging from 200 ms to 220 ms.

retardation without modulation suggests that the stress at the center of the modified region changes irregularly (for instance, from 100 ms to 200 ms). Although the plot of phase retardation with temporal energy modulation looks like a larger width of vibration than that without modulation, an apparent decrease in phase retardation was observed in the plot with temporal energy modulation. Furthermore, the relaxation of phase retardation was repeated at the modulation frequency of the sinusoidal wave. Finally, the phase retardation decreased by approximately 20 percent. Such a periodic relaxation of the phase retardation leads to a reduced stress concentration at the center of the modified region.

Since the generation of plasma and its movement are related to the stress distribution leading to the smoothness of the modified region, it is important to control the plasma movement. Assuming the generated plasma acts as a complete conductor, such momentarily changing plasma reflects the incident laser pulses. We have also simulated the plasma motion based on the calculated electric field component by the finite-difference time-domain (FDTD) method (COMSOL Multiphysics). The electric field was computed by the electromagnetic waves, frequency domain interface using the wave optics module. The electric field of a Gaussian distributed light propagating and focusing inside the 2D simulation box with the refractive index of alkali glass ($n = 1.45$) was computed by the electromagnetic waves, frequency domain interface using the wave optics module. The input electric field intensity with or without energy modulation was set to be $\frac{1}{2}(1 + \sin 2\pi x)$ or 1 V/m, respectively. To prevent the reflection at the boundary, the boundary condition of the simulation box was set to be the scattering boundary condition. Furthermore, by providing the boundary condition of a perfect electric conductor in the plasma region, we reproduced the plasma reflection of the electromagnetic waves. In the simulation, the threshold of the electric field intensity for plasma reflection during laser pulses focusing was set. This threshold was determined from the experiments whether a molten region was formed or not inside a glass sample by changing the laser intensity. We assumed that the plasma generation is the trigger of the formation of molten region in the vicinity of the focus. In our case, the intensity threshold for the alkali silicate glass was 1.98 μJ under the picosecond laser focusing with the pulse repetition rate of 500 kHz. In addition, due to a low thermal diffusion coefficient of glass, it is reasonably suggested that the temperature around the plasma generated region remains sufficiently high and accumulated heat is not diffused in a short time. In our calculation, we used the thermal diffusion coefficient of $0.46\,\mu m^2/\mu s$[3]. Although the plasma lifetime (~100 ps) is much shorter than the pulse interval (2 μs), we assumed the generated plasma presents in the glass until two subsequent laser pulses by the influence of the thermally excited electron. Based on the calculation of the electric field intensity during each laser pulse irradiation, we treated the region in which the electric field intensity exceeds the threshold for plasma generation as a complete conductor.

A time-sequential simulation of the electric field distribution is shown in Fig. 5. In this simulation, the pulse energy was set to be 5 μJ. Compared with the experimental observation of plasma movement without temporal energy modulation [Fig. 1(d)], we can consider that this simulation reproduces the plasma movement qualitatively from two viewpoints: (1) shape change of plasma during plasma movement, and (2) simultaneous generation of two plasma spots [Fig. 5(b)]. Although the amount of plasma movement is different from the experiments, the intermittent plasma generation during laser focusing with energy modulation [Fig. 1(c)] has also been qualitatively reproduced by this simulation [Fig. 5(a)]. The effort to improve the accuracy, such as determination of the absorption coefficient considering temperature change, should be required.

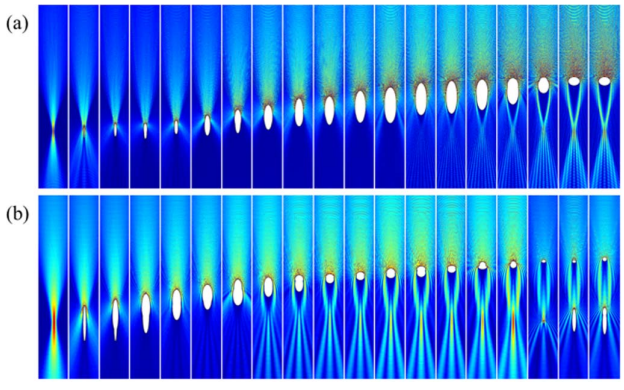

Fig. 5. Simulation of the electric field distribution inside the alkali silicate glass induced by the focused paraxial Gaussian laser beams (a) with and (b) without pulse energy modulation. The time sequential calculation of the electric field distribution is successively shown from left to right. In the calculation, the region in which the electric field intensity exceeded a threshold for plasma generation (white area) was set to be a perfect conductor.

In conclusion, the fundamental element of the difference in the modification induced by picosecond laser pulses with and without temporal energy modulation is the stress relaxation caused by the plasma generation and its movement. Even for picosecond laser pulses, by modulating the pulse energy with adequate frequency according to the thermal diffusion coefficient of materials, the induced stress distribution can be intentionally relaxed to the degree of that for femtosecond laser pulses. We have also qualitatively reproduced the plasma movement by FDTD simulation. Apart from the basic understanding, this technique for preventing the stress distribution opens new possibility for picosecond laser micromachining.

We would like to thank Mr. K. Ikuo from Photoron Ltd. for his help with using the high-speed 2D polarization camera. This work was partially supported by JSPS KAKENHI (Nos. JP17H03040 and 20H02656).

References

1. C. B. Schaffer, J. F. García, and E. Mazur, Appl. Phys. A **76**, 351 (2003).
2. S. M. Eaton, H. Zhang, P. R. Herman, F. Yoshino, L. Shah, J. Bovatsek, and A. Y. Arai, Opt. Express **13**, 4708 (2005).
3. M. Shimizu, M. Sakakura, M. Ohnishi, Y. Shimotsuma, T. Nakaya, K. Miura, and K. Hirao, J. Appl. Phys. **108**, 073533 (2010).
4. I. Miyamoto, Y. Okamoto, R. Tanabe, and Y. Ito, Phys. Procedia **56**, 973 (2014).
5. T. Tamaki, W. Watanabe, J. Nishii, and K. Itoh, Jpn. J. Appl. Phys. **44**, L687 (2005).
6. S. Richter, S. Döring, A. Tünnermann, and S. Nolte, Appl. Phys. A **103**, 257 (2011).
7. R. M. Carter, J. Chen, J. D. Shephard, R. R. Thomson, and D. P. Hand, Appl. Opt. **53**, 4233 (2014).
8. K. Cvecek, S. Dehmel, I. Miyamoto, and M. Schmidt, Int. J. Extrem. Manuf. **1**, 042001 (2019).
9. C. B Schaffer, A. Brodeur, and E. Mazur, Meas. Sci. Technol. **12**, 1784 (2001).
10. R. Knechtel, Microsyst. Technol. **12**, 63 (2005).
11. M. Sun, U. Eppelt, W. Schulz, and J. Zhu, Opt. Mater. Express **3**, 1716 (2013).
12. B. C. Stuart, M. D. Feit, A. M. Rubenchik, B. W. Shore, and M. D. Perry, Phys. Rev. Lett. **74**, 2248 (1995).
13. I. Miyamoto, K. Cvecek, and M. Schmidt, Opt. Express **19**, 10714 (2011).
14. I. Miyamoto, Y. Okamoto, R. Tanabe, Y. Ito, K. Cvecek, and M. Schmidt, Opt. Express **24**, 25718 (2016).
15. I. H. W. Nordin, Y. Okamoto, A. Okada, T. Takekuni, and T. Sakagawa, Appl. Phys. A **122**, 492 (2016).
16. A. Nakamura, M. Sakakura, Y. Shimotsuma, and K. Miura, J. Laser Micro/Nanoen. **12**, 126 (2017).
17. S. J. Sheldon, L. V. Knight, and J. M. Thorne, Appl. Opt. **21**, 1663 (1982).
18. M. Sakakura, M. Terazima, Y. Shimotsuma, K. Miura, and K. Hirao, Opt. Express **15**, 16800 (2007).
19. T. T. Fernandez, J. Siegel, J. Hoyo, B. Sotillo, P. Fernandez, and J. Solis, J. Phys. D **48**, 155101 (2015).
20. D. von der Linde and H. Schüler, J. Opt. Soc. Am. B **13**, 216 (1996).
21. K. Bergner, B. Seyfarth, K. A. Lammers, T. Ullsperger, S. Döring, M. Heinrich, M. Kumkar, D. Flamm, A. Tünnermann, and S. Nolte, Appl. Opt. **57**, 4618 (2018).
22. G. Sun, H. B. Jiang, Y. Liu, Y. H. Zhou, H. Yang, and Q. H. Gong, Chin. Phys. Lett. **23**, 189 (2006).
23. M. Sun, U. Eppelt, S. Russ, C. Hartmann, C. Siebert, J. Zhu, and W. Schulz, Opt. Express **21**, 7858 (2013).
24. C. Corbari, A. Champion, M. Gecevičius, M. Beresna, Y. Bellouard, and P. G. Kazansky, Opt. Express **21**, 3946 (2013).
25. D. Du, X. Liu, G. Korn, J. Squier, and G. Mourou, Appl. Phys. Lett. **64**, 3071 (1994).
26. M. Sakakura, M. Terazima, Y. Shimotsuma, K. Miura, and K. Hirao, Opt. Express **15**, 5674 (2007).